David Ho,[1] Xin Zhao,[1] Lin Yan,[1] Chujun Yuan,[1] Haihong Zong,[2] Dorothy E. Vatner,[1] Jeffery E. Pessin,[2] and Stephen F. Vatner[1]

Adenylyl Cyclase Type 5 Deficiency Protects Against Diet-Induced Obesity and Insulin Resistance

Diabetes 2015;64:2636–2645 | DOI: 10.2337/db14-0494

Adenylyl cyclase type 5 knockout (AC5KO) mice have increased longevity and share a similar phenotype with calorie-restricted wild-type (WT) mice. To determine the in vivo metabolic properties of AC5 deficiency, we compared the effects of standard diet (SD) and high-fat diet (HFD) on obesity, energy balance, glucose regulation, and insulin sensitivity. AC5KO mice on SD had reduced body weight and adiposity compared with WT mice. Blood cholesterol and triglyceride levels were also significantly reduced in AC5KO mice. Indirect calorimetry demonstrated increased oxygen consumption, respiratory exchange ratio, and energy expenditure in AC5KO compared with WT mice on both SD and HFD. AC5KO mice also displayed improved glucose tolerance and increased whole-body insulin sensitivity, accompanied by decreased liver glycogen stores. Euglycemic-hyperinsulinemic clamp studies confirmed the marked improvement of glucose homeostasis and insulin sensitivity in AC5KO mice primarily through increased insulin sensitivity in skeletal muscle. Moreover, the genes involved in mitochondrial biogenesis and function were significantly increased in AC5KO skeletal muscle. These data demonstrate that deficiency of AC5 protects against obesity, glucose intolerance, and insulin resistance, supporting AC5 as a potential novel therapeutic target for treatment of obesity and diabetes.

Adenylyl cyclase (AC) converts ATP to cAMP, an important second messenger regulating biological function throughout the body. When type 5 AC (AC5), one of nine AC isoforms, is disrupted (knocked out [KO]) in mice, the AC5KO mice live a third longer than wild type (WT) mice (1). Previous studies from our group have also established that AC5 deficiency results in reduced oxidative stress (1), protects against heart failure (2), and increases longevity with reduced weight gain similar to that observed in calorie-restricted mice (1,3). In fact, mechanisms linking calorie restriction and AC5 deficiency are so close that when calorie restriction is applied to AC5KO mice, they no longer live longer and actually die within a month (3).

Calorie restriction is an excellent therapeutic approach for diabetic (4) and obese (5) patients, but compliance with this regimen is difficult. Accordingly, a novel mechanism mimicking calorie restriction translated to the clinic would be extremely important. Thus, the goal of this investigation was to determine the extent to which the AC5KO mice are protected against glucose intolerance, insulin resistance, dyslipidemia, and obesity on both a standard diet (SD) and a high-fat diet (HFD) and whether AC5 inhibition could be a novel mechanism for diabetes and obesity therapy.

RESEARCH DESIGN AND METHODS

Generation of AC5KO Mice

C57BL/6J background mice with systemic AC5 gene deficiency were developed as previously described (6). The AC5KO mice were generated by crossing heterozygotes, $AC5^{-/+}$, to generate $AC5^{-/-}$ and $AC5^{+/+}$ WT littermates as controls. Pups were weaned at 28 days of age and housed individually to allow for measures of food intake in a pathogen-free facility under a 12:12 h light: dark cycle with access to water and food ad libitum. The

[1]Departments of Cell Biology and Molecular Medicine and Medicine, New Jersey Medical School, Rutgers University, Newark, NJ
[2]Departments of Medicine and Molecular Pharmacology, Albert Einstein College of Medicine, Bronx, NY
Corresponding author: Stephen F. Vatner, vatnersf@njms.rutgers.edu.

Received 26 March 2014 and accepted 17 February 2015.

This article contains Supplementary Data online at http://diabetes.diabetesjournals.org/lookup/suppl/doi:10.2337/db14-0494/-/DC1.

D.H., X.Z., and L.Y. contributed equally to this study.

6- to 12-week-old AC5KO and WT mice were studied on SD and also after 100 days of HFD, containing 60% of kilocalories from fat (F3282; Bio-Serv, Frenchtown, NJ). The source of fat includes linoleic, linolenic, saturated, monounsaturated, and saturated fatty acids (Supplementary Table 1). Body weight and food consumption (the difference between the amount of assigned food and the leftover food after 3–4 days) were recorded twice a week. Age- and sex-matched mice on SD were also followed as a control. At the end of 100 days on the HFD, the animals were killed. Rate of weight gain was monitored for the entire study period. The weight gain efficiency was calculated based on the body weight increase normalized by total calorie consumption. The experiments performed at Rutgers–New Jersey Medical School were approved by the Institutional Animal Care and Use Committee, and all animals were maintained in accordance with the guidelines in the Guide for the Care and Use of Laboratory Animals (7).

Fasting Glucose, Lipid Profile, and Insulin Levels and Insulin Resistance

After a 6-h fast, animals were anesthetized with 290 mg/kg i.p. Avertin, and the blood samples were drawn for fasting glucose, lipid profile, and insulin levels. The glucose was measured with a glucometer (Accu-Chek Aviva; Roche Diagnostics). Blood insulin was measured by ELISA (Crystal Chem, Dovers Grove, IL). The total cholesterol was measured by a Cholesterol Quantification Kit (Abcam, Cambridge, MA), the triglycerides were measured using CardioChek PA Analyzer (Fisher Scientific), and the free fatty acids were analyzed using an ELISA assay (WAKO Chemical GmbH). The insulin resistance, expressed as HOMA of insulin resistance (HOMA-IR), was calculated as follows: (fasting glucose $\times$ insulin)/22.5.

Calculation of Adiposity Index

Gonadal, perirenal, retroperitoneal, and inguinal fat pads were isolated and weighed. The adiposity index was calculated using total adipose depot weight divided by live body weight and then multiplied by 100.

Indirect Calorimetry

At the end of the 100-day SD and HFD periods, the mice were individually housed in separate metabolic chambers (Accuscan Instruments Inc.) with ad libitum access to food and water. The chambers were placed into a controlled environment with regulated temperature and 12-h day/night cycles. Oxygen consumption and carbon dioxide production were recorded every 10 min for 48 h, and respiratory exchange ratio (RER) and energy expenditure (EE) were calculated.

Glucose Tolerance Test

On a monthly basis, mice were fasted for 6 h prior to initiation of the glucose tolerance test (8). A blood sample was collected from a venous tail puncture, and blood glucose was measured for basal glucose measurement with an Accu-Chek glucometer. A dose of dextrose (1 g/kg body wt i.p.) was injected, and blood was drawn at 15, 30, 60, 120, and 180 min for blood glucose determination. The area under the glucose tolerance curve was calculated and compared. Prior to killing, mice were again fasted, and terminal blood was collected for glucose and insulin levels using the same methods as described above.

Insulin Tolerance Test

Similar to the glucose tolerance test, mice were fasted for 6 h prior to initiation of the insulin sensitivity test (8). A blood sample was drawn at the end of the fasting period for basal glucose measurement with the Accu-Chek glucometer. A dose of 1 unit/kg i.p. Humalog (Eli Lilly) was injected, and blood was drawn at 15, 30, 60, 90, and 120 min for blood glucose determination. The areas above the curve were calculated and compared. Because the AC5KO mice were more sensitive to insulin, there was not full recovery over the 120-min time. Therefore, we extrapolated the data to baseline to calculate the area above the curve for all the animals.

Euglycemic-Hyperinsulinemic Clamp

After a 12-h fast, euglycemic-hyperinsulinemic clamps were conducted in conscious mice as previously described (9,10). The 2-h euglycemic-hyperinsulinemic clamp studies were conducted with a continuous infusion of human insulin (4 mU/kg/min) and a variable infusion of 25% glucose to maintain glucose at 90 mg/dL. Insulin-stimulated whole-body glucose metabolism was estimated using a continuous infusion of [3-^{3}H]glucose (0.1 μCi/min; PerkinElmer Life Sciences). For determination of the rate of basal glucose turnover, [3-^{3}H]glucose (0.05 μCi/min) was infused for 2 h (basal period) with a 5-μCi bolus before starting the euglycemic-hyperinsulinemic clamp, and a blood sample was taken at the end of this basal period. For assessment of insulin-stimulated tissue-specific glucose uptake, 2-deoxy-D-[1-^{14}C]glucose (2-[^{14}C]DG) was administered as a bolus (10 μCi) 75 min after the start of the clamp. Blood samples were taken at time 0 and every 10 min for 80–120 min through the carotid artery. For estimation of basal muscle glucose uptake, 2-[^{14}C]DG glucose was infused with isotonic saline. During the clamp, plasma glucose was monitored using 2 μL blood by glucose meter (Precision Xtra; Abbot, Bedford, MA). Plasma [3-^{3}H]glucose, 2-[^{14}C]DG glucose, and $^{3}H_2O$ concentration were measured as previously described (9). After the euglycemic-hyperinsulinemic clamp studies, the animals were anesthetized and tissues were collected and immediately frozen at −80°C for the measurement of glucose uptake.

Histology

Liver and fat pads were collected from the AC5KO and WT mice fed with both SD and HFD and were fixed with 10% formalin. Paraffin-embedded samples were sectioned at 6-μm thickness. The visceral fat pads, which include perirenal, retroperitoneal, and gonadal fat pads, were

stained with hematoxylin–eosin, and the liver had periodic acid Schiff staining. Adipocyte cell size and hepatic glycogen stores were quantified under ×200 magnification using Image-Pro Plus software.

Quantitative RT-PCR

Specific primers and probes (derived with FAM and TAMRA [IDT DNA Company]) were designed for the transcripts of interest. The optimal combination of primers and probes for a quantitative PCR assay was determined with the Primer Express software (Applied Biosystems). After reverse transcription of the mRNA of interest from 50 ng total RNA, the cDNA was used for quantitative PCR (40 cycles of a 10-s step at 95°C and a 1-min step at 60°C) using the SYBR Green method on a 7700 ABI-Prizm Sequence Detector (Applied Biosystems, Foster City, CA). Values are reported per cyclophilin transcript to correct for sample-to-sample RNA loading variations. The sequence of the primers is listed in Supplementary Table 2.

Data Analysis and Statistics

Data are presented as mean ± SEM. Statistical comparisons among groups ($n \geq 3$) were calculated using two-way ANOVA. Comparisons between two groups were calculated using a two-tailed Student t test. P values of <0.05 were considered significant.

RESULTS

AC5 Deficiency Reduces HFD-Induced Obesity

Compared with WT mice, AC5KO mice maintained on either SD or HFD weighed less (Fig. 1*A*), despite increased calorie consumption, resulting in reduced weight gain efficiency in the AC5KO compared with WT mice (Fig. 1*B*). HFD increased body weight of AC5 WT mice by 14.8 ± 1.4% compared with 9.6 ± 1.0% for AC5KO mice, $P <$ 0.05. Percent body fat as measured by adiposity index was significantly lower in the AC5KO mice maintained on either SD or HFD (Fig. 1*C*). The decreased adiposity was reflected by a decrease in visceral fat pad mass (Fig. 1*D*) and inguinal fat pad mass (data not shown). With SD, the

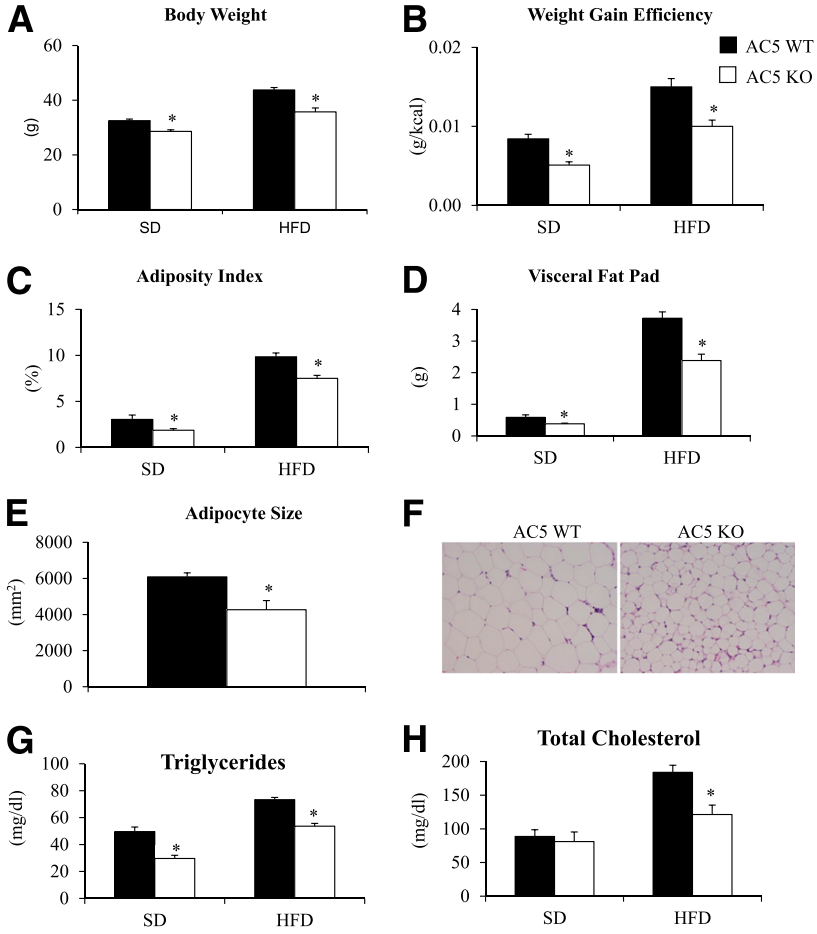

Figure 1—Genetic disruption of AC5 protected mice from obesity with SD or when stressed with HFD for 100 days. In AC5KO mice, the body weight was less (*A*), and the weight gain efficiency was also less (*B*), compared with WT mice. Adiposity index (*C*) and visceral fat pad weights (*D*) were lower in KO mice with both SD and HFD, accompanied by smaller visceral adipocyte cell size (*E* and *F*). The protection was further supported with lower triglycerides (*G*) in AC5KO mice with both diets and lower total cholesterol with HFD (*H*). Results are expressed as the mean ± SEM. *$P < 0.05$ vs. WT, n = 5–6 per group.

visceral fat was less ($P < 0.05$) in AC5KO mice (0.39 ± 0.02 vs. 0.59 ± 0.05 g in WT). With HFD, the visceral fat increased significantly ($P < 0.05$) in WT (3.7 ± 0.2 g) but less in AC5KO (2.4 ± 0.2 g) mice (Fig. 1*D*). Visceral adipocyte size was also significantly smaller in AC5KO mice with HFD (Fig. 1*E*). Histologically, AC5KO mice displayed smaller adipocytes (Fig. 1*F*) with a greater number of adipocytes smaller than 3,000 μm^2, while WT mice had more adipocytes larger than 3,000 μm^2. The decreased body weight and lower obesity in AC5KO mice were further supported by significantly lower triglycerides under both SD- and HFD-fed conditions (Fig. 1*G*) and 34% reduction in total cholesterol under HFD feeding (Fig. 1*H*).

AC5 Deficiency Enhances EE

It is well recognized that increased metabolic rate, as observed with chronic exercise (11) or with hyperthyroidism (12), is effective in reducing obesity, protecting against glucose intolerance and insulin resistance (13,14). Indirect calorimetry assessed oxygen consumption, CO_2 production, and RER and calculated EE. Each one of these measurements was greater in AC5KOs than WTs on SD and HFD (Fig. 2). The increase in RER reflects the increase in glucose utilization and is consistent with the lower fasting blood glucose levels (Fig. 3*D*), whereas the increase in EE is consistent with an enhanced metabolic rate (3) (Fig. 2*C* and *D*). For clarity, the averaged light and dark cycle data are shown in Fig. 2. However, the increases in these parameters tended to be greater in the dark cycle. For example, on HFD there were greater increases in AC5KO, $P < 0.05$, in the dark cycle (15.1 ± 1.0 kcal/kg/h in AC5KO vs. 9.6 ± 0.3 kcal/kg/h in WT mice, $P < 0.05$) compared with the increases in the light cycle (11.1 ± 1.0 kcal/kg/h in AC5KO vs. 8.1 ± 0.7 kcal/kg/h in WT mice). Although the energy expenditure was higher in KO mice compared with WT mice, under both SD and HFD, the body temperature was not significantly different in either the dark or light cycles.

AC5 Deficiency Improves Insulin Sensitivity and Protects Against HFD-Induced Insulin Resistance

In parallel with the reduction in adiposity and improvement in energy balance, the AC5KO mice on SD also displayed lower fasting glucose levels (Fig. 3*D*) with improved glucose tolerance (Fig. 3*A* and *C*). Similarly, the AC5KO on HFD also had an improved glucose tolerance (Fig. 3*B* and *C*). The lower fasting glucose was accompanied by significantly lower hepatic glycogen stores under HFD (Fig. 3*E* and *F*). To determine whether the improved glucose tolerance was a result of increased insulin sensitivity, we next performed insulin tolerance tests. Both on SD and on HFD, the AC5KO mice had significantly improved insulin tolerance (Fig. 4). Accordingly, we assessed the fasting insulin levels and HOMA-IR in the HFD-fed mice. Consistent with an increase in insulin sensitivity, fasting insulin levels were lower in the AC5KO mice with a lower HOMA-IR (Fig 4*D* and *E*). As the use of HOMA-IR to assess insulin sensitivity in mice is highly variable (15,16), we directly determined insulin sensitivity using conscious nonstressed euglycemic-hyperinsulinemic clamp analyses. The glucose infusion rate needed to maintain euglycemia was significantly elevated in the AC5KO mice compared with WT mice and resulted from an increased whole-body insulin-stimulated glucose uptake (Fig. 5*A* and *B*). The tissue-specific insulin sensitivity was also assessed using radioactive 2-deoxyglucose during the euglycemic-hyperinsulinemic clamps and demonstrated a skeletal muscle–specific increase in glucose uptake in the AC5KO mice (Fig. 5*C*). However, there were no significant

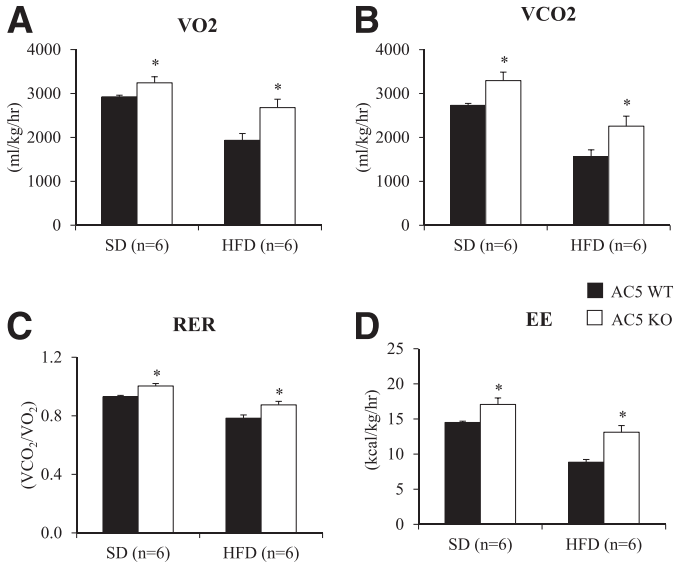

Figure 2—The mice were placed in a metabolic chamber for 48 h. The average oxygen consumption (VO_2) (*A*) and CO_2 production (VCO_2) (*B*) and calculated RER (*C*) and EE (*D*) were significantly higher in AC5KO compared with WT mice with both diets. Results are expressed as the mean ± SEM. *$P < 0.05$ vs. WT, $n = 5–7$ per group.

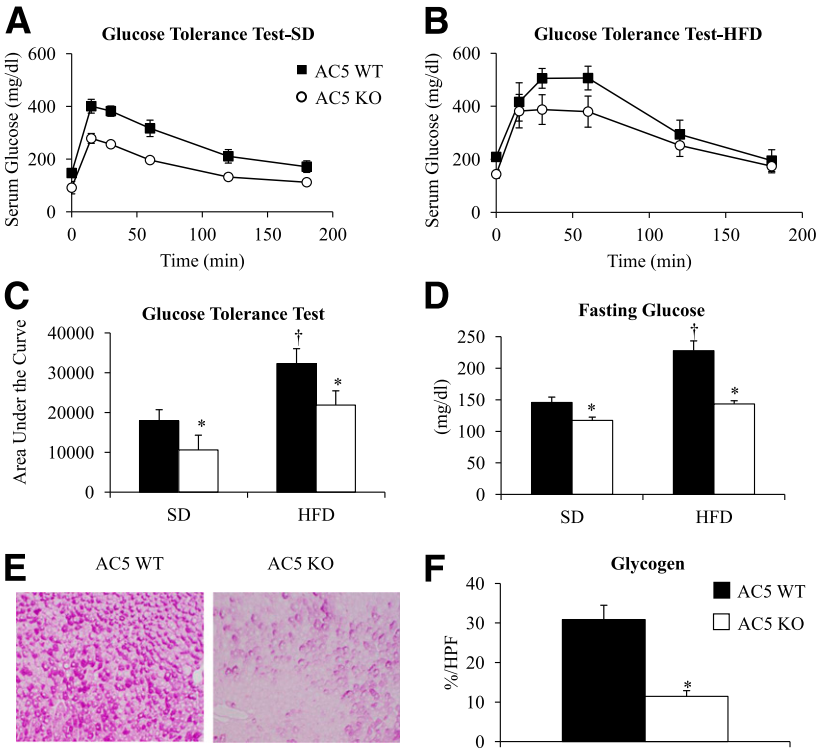

Figure 3—Compared with WT mice, AC5KO mice display improved glucose tolerance with SD and HFD as shown in curves (*A* and *B*) and area under the curves (*C*) and reduced fasting glucose (*D*). Representative image of hepatic glycogen staining (*E*) showed significantly less glycogen stores in AC5KO (*F*). Glycogen was quantified and presented as percent per high power field (HPF). Results are expressed as the mean ± SEM. n = 6–8 per group. *P < 0.05 vs. WT, †P < 0.05 vs. WT on SD.

differences in AC5KO or WT mice in adipose tissue or cardiac muscle glucose uptake (Fig. 5*D* and *E*) or the ability of insulin to suppress hepatic glucose output (Fig. 5*F*).

AC5KO Mice Have Increased Expression of Mitochondrial Metabolic Genes in Skeletal Muscle

The improvement in energy balance and skeletal muscle glucose uptake correlated with the expression of mitochondria markers indicative of increased mitochondria function (ATPG1, citrate synthase, cyclooxygenase IV [COX IV], and cytochrome C) and protection against mitochondria oxidative stress (MnSOD, nuclear respiratory factor-1 [Nrf-1], and NADH dehydrogenase [ubiquinone] 1 alpha subcomplex, 2 [Ndufa2]), respectively (Fig. 6*A* and *B*). In the gastrocnemius muscle of the AC5KO animals, ATP, COX IV, and citrate synthase expression were 47 ± 17%, 72 ± 7%, and 37 ± 14% higher (P < 0.05) compared with WT mice. These data suggest that improved mitochondrial metabolism in skeletal muscle is the likely mechanism responsible for the enhancement of glucose tolerance and insulin sensitivity in the AC5KO mice. As increased skeletal muscle mitochondrial metabolism is associated with white adipose tissue browning (17), we also examined the expression of several beige adipocyte markers that were all increased in visceral adipose tissue of the AC5KO mice (Fig. 6*C*). These data suggest that part of the improved energy balance phenotype of the AC5KO mice may result from increased beige fat thermogenesis.

DISCUSSION

The major finding of this investigation is that the AC5KO mouse, challenged with an HFD, is resistant to glucose intolerance, insulin resistance, and obesity, thereby identifying a novel target for the growing epidemic of diabetes and obesity. It is well established that chronic feeding of mice with an HFD mimics many of the phenotypes associated with metabolic syndrome including obesity, insulin resistance, and glucose intolerance (18,19). Indeed, the WT mice fed an HFD became obese, glucose intolerant, and insulin resistant, whereas the AC5KO mice on the HFD demonstrated significant reductions in adiposity resulting from a decrease in both subcutaneous and visceral adipocyte cell size. The protection against visceral adipose tissue expansion is of particular importance, since the role of visceral fat in diabetes and heart disease has been well established (20,21).

The genetic deficiency of AC5 not only protects against obesity but also protects against glucose intolerance and insulin resistance, which are the signature features of type 2 diabetes. Euglycemic-hyperinsulinemic clamp studies not only confirmed the protection against HFD-induced insulin resistance but also demonstrated a selective protection in skeletal muscle glucose uptake along with reduced hepatic glycogen stores suggesting an increased energy demand. These data suggest that one mechanism by which the AC5KO mouse is protected involves changes in metabolism.

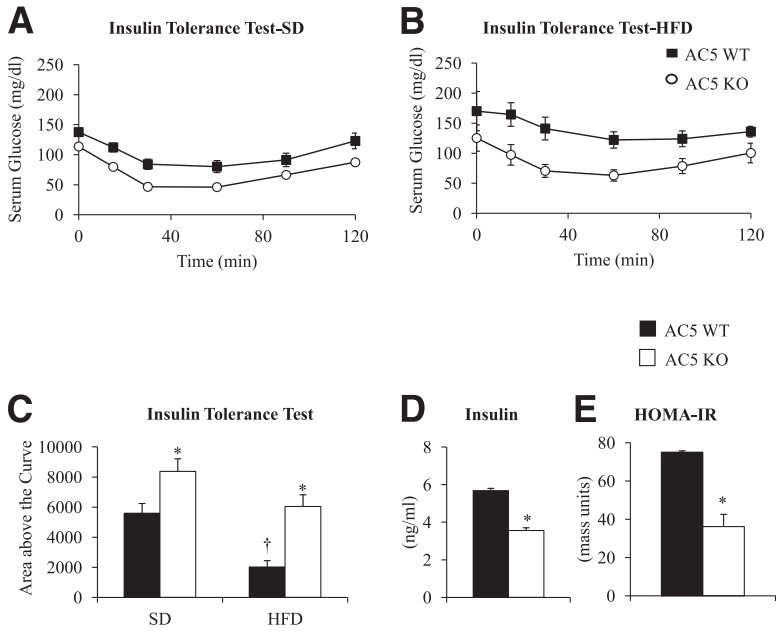

Figure 4—AC5KO mice display enhanced insulin sensitivity with SD (*A* and *C*) and HFD (*B* and *C*). The lower fasting insulin (*D*) in KO mice together with lower fasting glucose (Fig. 3*D*) yields a significantly lower HOMA-IR (*E*) compared with WT mice. Results are expressed as the mean ± SEM. **P* < 0.05 vs. WT, †*P* < 0.05 vs. WT on SD, *n* = 6–13 per group.

Accordingly, we monitored the mice in a metabolic chamber for 48 h. We found that total body oxygen consumption was increased in AC5KO compared with WT mice, more at night than in the day, corresponding to the nocturnal activity of mice. With both SD and HFD, the RER was higher in KO mice compared with the WT mice, which suggests increased glucose metabolism and is consistent with the lower fasting blood glucose.

We also demonstrated that AC5 deficiency primarily enhances glucose uptake in skeletal muscle. The optimal utilization and balance between carbohydrate and fatty acid metabolism are critical elements necessary for appropriate energy homeostasis and disturbances in the integrated physiology of fuel switching, which occurs with obesity, insulin deficiency, and type 2 diabetes. Fuel switching by the skeletal muscle means shifting between utilization of carbohydrate and fat as an oxidative source and is an important mechanism in maintaining homeostasis of these fuel substrates. The data presented in this study strongly support the hypothesis that AC5 deficiency improves skeletal muscle glucose metabolism and increases EE through increased glucose utilization and mitochondrial function with reduced oxidative stress. Indeed, reduced oxidative stress was found to be an important mechanism in mediating the longevity and protection against catecholamine stress in AC5KO mice (1,22).

An important mechanism by which metabolism is increased, resulting in protection against diabetes and obesity, involves increased brown adipose tissue (23). We did not observe an increase in intrascapular brown fat in the AC5KO mice. However, we did observe increases in genes responsible for white fat browning (beige adipocytes) in AC5KO, such as UCP-1 and Pparγ1 (Fig. 6*C*). The apparent increase in beige adipocytes likely accounts for the increase in EE and likely contributes to the overall improved glucose homeostasis in the AC5KO mice. Interestingly, there appear to be two general mechanisms for increased adipocyte browning: activation of sympathetic tone, e.g., via cold adaptation, or through the protection of circulating factors derived from skeletal muscle, e.g., exercise (24,25). As sympathetic tone activation is mediated by elevation of cell-autonomous cAMP levels, it is highly unlikely that the beige adipocyte precursors display elevated cAMP levels after AC5 deficiency. As increased skeletal muscle mitochondrial function can also increase white adipose tissue browning via circulating factors, we speculate that the AC5KO enhancement of skeletal muscle metabolism likely accounts for the observed secondary effects on browning.

It was unexpected to find that the body temperature was similar in the AC5 WT and AC5KO mice, since in most cases animals with higher EE and more white fat browning have higher temperatures (26,27). However, the AC5KO is not a typical animal model of higher EE. Most animal models with higher EE have reduced life span (11,28), whereas mouse models of increased longevity typically have lower body temperature (29,30). The AC5KO model is unique because it has higher EE with prolonged life span (1), with no significant change in body temperature.

Since the AC5KO mice have reduced AC activity and thus reduced cAMP, it is obvious to ask whether reduced cAMP levels contribute to this metabolic phenotype. Prior studies examining agents or mechanisms with reduced cAMP have been controversial in their effect on reducing

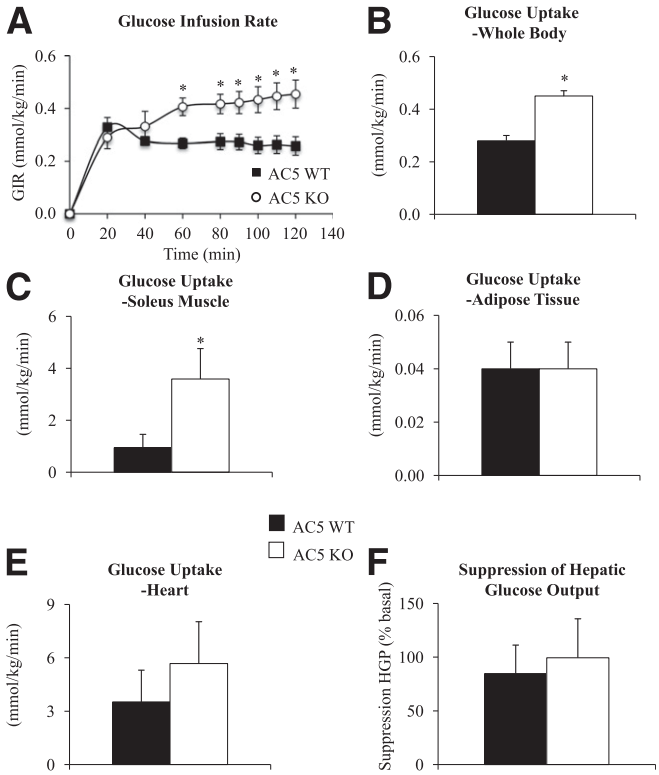

Figure 5—In AC5KO mice with SD, euglycemic-hyperinsulinemic clamps demonstrated significantly increased glucose infusion rate necessary to maintain euglycemia (*A*) and increased glucose uptake in the whole body (*B*) and in skeletal muscle (*C*) but not for adipose tissue (*D*) or heart (*E*). The suppression of hepatic glucose output was similar between the groups (*F*). Results are expressed as the mean ± SEM. *$P < 0.05$ vs. WT, $n = 5$ per group.

glucose and insulin intolerance. Some studies showed that upregulation of cAMP results in improvement in glucose and insulin tolerance (31–34). For example, the G-protein–coupled receptor 119 (GPR119), which is predominantly expressed in pancreatic β-cells, has recently been identified as a promising antidiabetic therapeutic target (35). GPR119 agonists have been shown to decrease blood glucose levels and preserve pancreatic β-cell function in type 2 diabetic rodent models (36) and in human subjects (37). The mechanism involves activation of GPR119 causing an increase in intracellular cAMP leading to enhanced glucose-stimulated insulin release and increased GLP-1 levels (38). In contrast, other studies showed that downregulation of cAMP results in improvement in glucose and insulin tolerance (31–34). For example, a recent study demonstrated that biguanides, such as metformin, protect against diabetes through a mechanism involving reduced glucagon-stimulated cAMP production in the liver (33), supporting the concept that reduction in cAMP may be the mechanism for the protection conferred by the AC5KO. However, inactivation of phosphodiesterase 4B in adipocytes results in increased steady-state levels of cAMP associated with a marked reduction in adiposity but with increased glucose homeostasis and insulin sensitivity (34) in contrast to the phosphodiesterase 3B KO mice (18). In further support of the position that simply decreasing cAMP cannot always be therapeutic for diabetes, β-adrenergic blockers, which inhibit the action of sympathetic stimulation to increase AC activity and cAMP, are widely used in the treatment of heart disease, which is commonly observed in diabetic patients, yet those β-adrenergic blockers, e.g., metoprolol, atenolol, or propranolol, all have an adverse effect on diabetes (31,39). Therefore, the reduced AC activity associated with inhibition of β-adrenergic signaling cannot be the sole mechanism for the salutary effects of the AC5KO in protecting against insulin and glucose intolerance. It may be that the beneficial effects of AC5 inhibition are AC isoform specific, since other AC isoform genetic models have not shown a beneficial role in insulin/glucose intolerance and obesity. For example, mice lacking type 3 AC exhibit obesity (40), and AC6KO mice on HFD do not demonstrate reduced adiposity. Furthermore, the AC5KO mice have extended longevity by ~33% and are protected against cancer (1,41), which may not be due simply to generalized reduction in cAMP, since other AC isoforms, when disrupted, do not have these effects or do not protect against diabetes or obesity (40).

Because of the strong association between obesity and diabetes, it is important to have a drug that controls both diabetes and body weight. Unfortunately, not many of the currently marketed drugs have both antidiabetic and

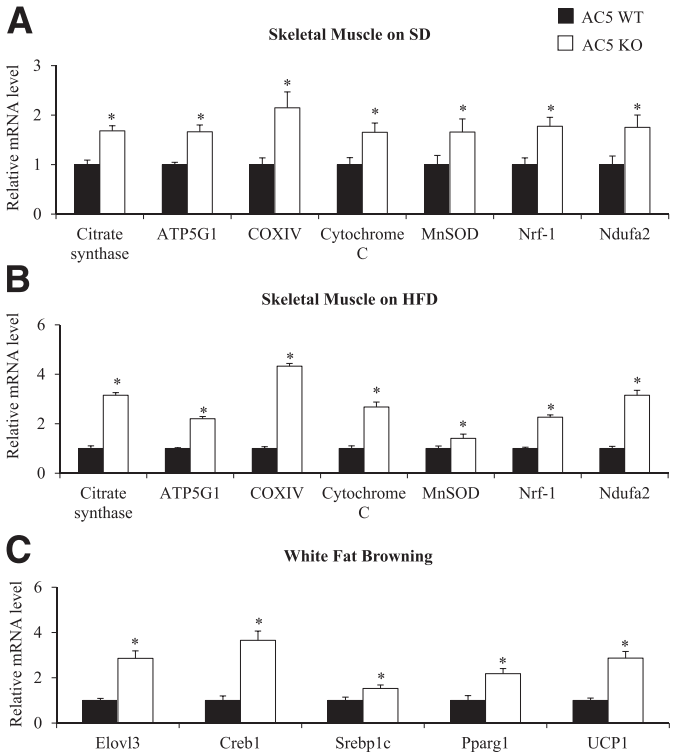

Figure 6—Genetic disruption of AC5 improved mitochondrial function in skeletal muscle with both SD (*A*) and HFD (*B*), determined by quantitative PCR. *C*: AC5KO mice also showed white fat browning with SD. Results are expressed as the mean ± SEM, and all values are expressed as percentage of WT with SD. *$P < 0.05$ vs. WT, $n = 5–6$ per group. The animal mRNA nomenclature is shown in Supplementary Table 2.

antiobesity properties. For instance, only metformin (42,43) and sodium-glucose cotransporter 2 inhibitors such as dapagliflozin and empagliflozin (44,45) have been shown to have both properties. Other medications, including dipeptidyl peptidase-4 inhibitors (46,47), sulfonylureas (48), and thiazolidinedione (49), have only antidiabetic properties. Other medical therapies, such as α-glucosidase inhibitors, were found to lower body weight and possibly improve insulin sensitivity, but no evidence is available as to whether they can improve glucose tolerance (50). Similarly, GLP-1 receptor agonists were shown to lower body weight and possibly improve glucose tolerance, without evidence of whether they can improve insulin sensitivity (51–53). Importantly, AC5 deficiency not only can lower body weight, but also can improve insulin sensitivity and glucose tolerance, thus providing intriguing evidence for further studies aimed at developing regulators of this pathway for the treatment of diabetes and obesity.

Recent genome-wide association studies have identified single nucleotide polymorphisms (SNPs) in the ADCY5 gene associated with increased type 2 diabetes risk (54–56). However, not all of these studies were consistent; whereas some suggest that ADCY5 is protective for diabetes (54,55,57), others found that ADCY5 impairs glucose and insulin metabolism (56,58). However, it is difficult in human genome studies to isolate the specific action of one gene as opposed to studies in mice, where one gene can be disrupted, as in the current investigation.

In summary, we have identified a novel molecular pathway, inhibition of AC5, as a potential therapeutic target for the growing epidemic of obesity and diabetes. Mice with AC5 deficiency are protected from diabetes and obesity under normal conditions and also in response to the stress induced by HFD. The mechanism appears not simply due to reduced cAMP but also due to enhanced energy balance and glucose metabolism in a manner akin to that previously reported for calorie restriction (9). The significance of this study extends beyond a new therapeutic mechanism for diabetes and obesity, which by itself is significant enough, to the concept of healthful aging. AC5KO is a longevity model, as these mice live a third longer than WT littermates (1). Longevity, per se, is not always beneficial, unless it is associated with healthful aging. Protection against diabetes and obesity, while extending longevity, is a hallmark of healthful aging, exemplified by the AC5KO model.

Acknowledgments. The authors are saddened by the premature passing of Dr. William Stanley, who gave advice for the HFD studies and metabolic assays.

Funding. This work was supported by National Institutes of Health grants 5-P01-AG-027211, 5-R21-HL-097264, 1-R01-HL-102472, 5-R01-HL-033107, 5-T32-HL-069752, 5-R01-HL-095888, 5-P01-HL-069020, 5-R01-HL-091781,

R01-HL-106511, R01-HL-093481, 1-R01-HL-119464, and 5-R37-DK-033823 and the Einstein Diabetes Center Research and Training Award (P60-DK-020541).

Duality of Interest. No potential conflicts of interest relevant to this article were reported.

Author Contributions. The concept and design of the study was the contribution of D.H., X.Z., L.Y., D.E.V., J.E.P., and S.F.V., who also wrote the manuscript. D.H., X.Z., and L.Y. performed the majority of experiments, analyzed the data, and summarized the literature. C.Y. performed experiments. H.Z., under the supervision of J.E.P., provided the data on glucose clamps.

References

1. Yan L, Vatner DE, O'Connor JP, et al. Type 5 adenylyl cyclase disruption increases longevity and protects against stress. Cell 2007;130:247–258
2. Iwatsubo K, Bravo C, Uechi M, et al. Prevention of heart failure in mice by an antiviral agent that inhibits type 5 cardiac adenylyl cyclase. Am J Physiol Heart Circ Physiol 2012;302:H2622–H2628
3. Yan L, Park JY, Dillinger JG, et al. Common mechanisms for calorie restriction and adenylyl cyclase type 5 knockout models of longevity. Aging Cell 2012;11:1110–1120
4. Lim EL, Hollingsworth KG, Aribisala BS, Chen MJ, Mathers JC, Taylor R. Reversal of type 2 diabetes: normalisation of beta cell function in association with decreased pancreas and liver triacylglycerol. Diabetologia 2011;54:2506–2514
5. Malandrucco I, Pasqualetti P, Giordani I, et al. Very-low-calorie diet: a quick therapeutic tool to improve β cell function in morbidly obese patients with type 2 diabetes. Am J Clin Nutr 2012;95:609–613
6. Okumura S, Kawabe J, Yatani A, et al. Type 5 adenylyl cyclase disruption alters not only sympathetic but also parasympathetic and calcium-mediated cardiac regulation. Circ Res 2003;93:364–371
7. National Research Council (US) Committee for the Update of the Guide for the Care and Use of Laboratory Animals. *Guide for the Care and Use of Laboratory Animals, 8th Edition*. Washington, DC, National Academies Press (US), 2011
8. Nomiyama T, Perez-Tilve D, Ogawa D, et al. Osteopontin mediates obesity-induced adipose tissue macrophage infiltration and insulin resistance in mice. J Clin Invest 2007;117:2877–2888
9. Zong H, Bastie CC, Xu J, et al. Insulin resistance in striated muscle-specific integrin receptor beta1-deficient mice. J Biol Chem 2009;284:4679–4688
10. Zong H, Wang CC, Vaitheesvaran B, Kurland IJ, Hong W, Pessin JE. Enhanced energy expenditure, glucose utilization, and insulin sensitivity in VAMP8 null mice. Diabetes 2011;60:30–38
11. Speakman JR, Selman C. Physical activity and resting metabolic rate. Proc Nutr Soc 2003;62:621–634
12. Kahaly GJ, Kampmann C, Mohr-Kahaly S. Cardiovascular hemodynamics and exercise tolerance in thyroid disease. Thyroid 2002;12:473–481
13. Nelson DW, Gao Y, Spencer NM, Banh T, Yen CL. Deficiency of MGAT2 increases energy expenditure without high-fat feeding and protects genetically obese mice from excessive weight gain. J Lipid Res 2011;52:1723–1732
14. Wan M, Easton RM, Gleason CE, et al. Loss of Akt1 in mice increases energy expenditure and protects against diet-induced obesity. Mol Cell Biol 2012;32:96–106
15. Ables GP, Perrone CE, Orentreich D, Orentreich N. Methionine-restricted C57BL/6J mice are resistant to diet-induced obesity and insulin resistance but have low bone density. PLoS ONE 2012;7:e51357
16. Weisberg SP, Hunter D, Huber R, et al. CCR2 modulates inflammatory and metabolic effects of high-fat feeding. J Clin Invest 2006;116:115–124
17. Kusminski CM, Scherer PE. Mitochondrial dysfunction in white adipose tissue. Trends Endocrinol Metab 2012;23:435–443
18. Ahrén B, Pacini G. Insufficient islet compensation to insulin resistance vs. reduced glucose effectiveness in glucose-intolerant mice. Am J Physiol Endocrinol Metab 2002;283:E738–E744
19. Parekh PI, Petro AE, Tiller JM, Feinglos MN, Surwit RS. Reversal of diet-induced obesity and diabetes in C57BL/6J mice. Metabolism 1998;47:1089–1096
20. Hamdy O, Porramatikul S, Al-Ozairi E. Metabolic obesity: the paradox between visceral and subcutaneous fat. Curr Diabetes Rev 2006;2:367–373
21. Nguyen-Duy TB, Nichaman MZ, Church TS, Blair SN, Ross R. Visceral fat and liver fat are independent predictors of metabolic risk factors in men. Am J Physiol Endocrinol Metab 2003;284:E1065–E1071
22. Lai L, Yan L, Gao S, et al. Type 5 adenylyl cyclase increases oxidative stress by transcriptional regulation of manganese superoxide dismutase via the SIRT1/FoxO3a pathway. Circulation 2013;127:1692–1701
23. Chondronikola M, Volpi E, Børsheim E, et al. Brown adipose tissue improves whole-body glucose homeostasis and insulin sensitivity in humans. Diabetes 2014;63:4089–4099
24. Lidell ME, Enerbäck S. Brown adipose tissue–a new role in humans? Nat Rev Endocrinol 2010;6:319–325
25. Ravussin E, Galgani JE. The implication of brown adipose tissue for humans. Annu Rev Nutr 2011;31:33–47
26. Bross R, Hoffer LJ. Fluoxetine increases resting energy expenditure and basal body temperature in humans. Am J Clin Nutr 1995;61:1020–1025
27. Fisher FM, Kleiner S, Douris N, et al. FGF21 regulates PGC-1α and browning of white adipose tissues in adaptive thermogenesis. Genes Dev 2012;26:271–281
28. Miquel J, Lundgren PR, Bensch KG, Atlan H. Effects of temperature on the life span, vitality and fine structure of Drosophila melanogaster. Mech Ageing Dev 1976;5:347–370
29. Van Raamsdonk JM, Meng Y, Camp D, et al. Decreased energy metabolism extends life span in Caenorhabditis elegans without reducing oxidative damage. Genetics 2010;185:559–571
30. Lyman CP, O'Brien RC, Greene GC, Papafrangos ED. Hibernation and longevity in the Turkish hamster Mesocricetus brandti. Science 1981;212:668–670
31. Fonseca VA. Effects of beta-blockers on glucose and lipid metabolism. Curr Med Res Opin 2010;26:615–629
32. Idevall-Hagren O, Barg S, Gylfe E, Tengholm A. cAMP mediators of pulsatile insulin secretion from glucose-stimulated single beta-cells. J Biol Chem 2010;285:23007–23018
33. Miller RA, Chu Q, Xie J, Foretz M, Viollet B, Birnbaum MJ. Biguanides suppress hepatic glucagon signalling by decreasing production of cyclic AMP. Nature 2013;494:256–260
34. Zhang R, Maratos-Flier E, Flier JS. Reduced adiposity and high-fat diet-induced adipose inflammation in mice deficient for phosphodiesterase 4B. Endocrinology 2009;150:3076–3082
35. Ohishi T, Yoshida S. The therapeutic potential of GPR119 agonists for type 2 diabetes. Expert Opin Investig Drugs 2012;21:321–328
36. Oshima H, Yoshida S, Ohishi T, et al. Novel GPR119 agonist AS1669058 potentiates insulin secretion from rat islets and has potent anti-diabetic effects in ICR and diabetic db/db mice. Life Sci 2013;92:167–173
37. Katz LB, Gambale JJ, Rothenberg PL, et al. Effects of JNJ-38431055, a novel GPR119 receptor agonist, in randomized, double-blind, placebo-controlled studies in subjects with type 2 diabetes. Diabetes Obes Metab 2012;14:709–716
38. Overton HA, Fyfe MC, Reynet C. GPR119, a novel G protein-coupled receptor target for the treatment of type 2 diabetes and obesity. Br J Pharmacol 2008;153(Suppl. 1):S76–S81
39. Jacob S, Balletshofer B, Henriksen EJ, et al. Beta-blocking agents in patients with insulin resistance: effects of vasodilating beta-blockers. Blood Press 1999;8:261–268
40. Wang Z, Li V, Chan GC, et al. Adult type 3 adenylyl cyclase-deficient mice are obese. PLoS ONE 2009;4:e6979
41. De Lorenzo MS, Chen W, Baljinnyam E, et al. 'Reduced malignancy as a mechanism for longevity in mice with adenylyl cyclase type 5 disruption'. Aging Cell 2014;13:102–110
42. Brufani C, Crino A, Fintini D, Patera PI, Cappa M, Manco M. Systematic review of metformin use in obese nondiabetic children and adolescents. Horm Res Pediatr 2013;80:78–85

43. Stumvoll M, Nurjhan N, Perriello G, Dailey G, Gerich JE. Metabolic effects of metformin in non-insulin-dependent diabetes mellitus. N Engl J Med 1995;333: 550–554
44. Brooks AM, Thacker SM. Dapagliflozin for the treatment of type 2 diabetes. Ann Pharmacother 2009;43:1286–1293
45. Kurosaki E, Ogasawara H. Ipragliflozin and other sodium-glucose cotransporter-2 (SGLT2) inhibitors in the treatment of type 2 diabetes: preclinical and clinical data. Pharmacol Ther 2013;139:51–59
46. Hanefeld M, Herman GA, Wu M, Mickel C, Sanchez M, Stein PP; Sitagliptin Study 014 Investigators. Once-daily sitagliptin, a dipeptidyl peptidase-4 inhibitor, for the treatment of patients with type 2 diabetes. Curr Med Res Opin 2007;23: 1329–1339
47. Rosenstock J, Sankoh S, List JF. Glucose-lowering activity of the dipeptidyl peptidase-4 inhibitor saxagliptin in drug-naive patients with type 2 diabetes. Diabetes Obes Metab 2008;10:376–386
48. Nathan DM, Buse JB, Davidson MB, et al.; Professional Practice Committee, American Diabetes Association; European Association for the Study of Diabetes. Management of hyperglycaemia in type 2 diabetes: a consensus algorithm for the initiation and adjustment of therapy. A consensus statement from the American Diabetes Association and the European Association for the Study of Diabetes. Diabetologia 2006;49:1711–1721
49. Fonseca V. Effect of thiazolidinediones on body weight in patients with diabetes mellitus. Am J Med 2003;115(Suppl. 8A):42S–48S
50. Nakamura K, Yamagishi S, Matsui T, Inoue H. Acarbose, an alpha-glucosidase inhibitor, improves insulin resistance in fructose-fed rats. Drugs Exp Clin Res 2005;31:155–159
51. Garber A, Henry R, Ratner R, et al.; LEAD-3 (Mono) Study Group. Liraglutide versus glimepiride monotherapy for type 2 diabetes (LEAD-3 Mono): a randomised, 52-week, phase III, double-blind, parallel-treatment trial. Lancet 2009; 373:473–481
52. Hollander P, Li J, Allen E, Chen R, Investigators CV; CV181-013 Investigators. Saxagliptin added to a thiazolidinedione improves glycemic control in patients with type 2 diabetes and inadequate control on thiazolidinedione alone. J Clin Endocrinol Metab 2009;94:4810–4819
53. Kelly AS, Metzig AM, Rudser KD, et al. Exenatide as a weight-loss therapy in extreme pediatric obesity: a randomized, controlled pilot study. Obesity (Silver Spring) 2012;20:364–370
54. Rees SD, Hydrie MZ, O'Hare JP, et al. Effects of 16 genetic variants on fasting glucose and type 2 diabetes in South Asians: ADCY5 and GLIS3 variants may predispose to type 2 diabetes. PLoS ONE 2011;6:e24710
55. Wagner R, Dudziak K, Herzberg-Schäfer SA, et al. Glucose-raising genetic variants in MADD and ADCY5 impair conversion of proinsulin to insulin. PLoS ONE 2011;6:e23639
56. Hodson DJ, Mitchell RK, Marselli L, et al. ADCY5 couples glucose to insulin secretion in human islets. Diabetes 2014;63:3009–3021
57. Dupuis J, Langenberg C, Prokopenko I, et al.; DIAGRAM Consortium; GIANT Consortium; Global BPgen Consortium; Anders Hamsten on behalf of Procardis Consortium; MAGIC investigators. New genetic loci implicated in fasting glucose homeostasis and their impact on type 2 diabetes risk. Nat Genet 2010;42:105–116
58. Windholz J, Kovacs P, Tönjes A, et al. Effects of genetic variants in ADCY5, GIPR, GCKR and VPS13C on early impairment of glucose and insulin metabolism in children. PLoS ONE 2011;6:e22101